JOURNAL OF ELECTROMAGNETIC ENGINEERING AND SCIENCE, VOL. 22, NO. 6, 678~685, NOV. 2022

https://doi.org/10.26866/jees.2022.6.r.137
ISSN 2671-7263 (Online) · ISSN 2671-7255 (Print)

C-Band GaN Dual-Feedback Low-Noise Amplifier MMIC with High-Input Power Robustness

Ha-Wuk Sung[1] · Seong-Hee Han[1] · Seong-Il Kim[2] · Ho-Kyun Ahn[2] · Jong-Won Lim[2] · Dong-Wook Kim[1,*]

Abstract

In this paper, using the 0.2 μm ETRI GaN HEMT process, we developed a C-band GaN dual-feedback low-noise amplifier MMIC for an RF receiver module that requires high-input power robustness. By applying a feedback microstrip line at the source of the transistor and series resistor-capacitor (RC) feedback between the gate and the drain of the transistor, we obtained stable amplifier operation and a compromised impedance trace for both input impedance matching and noise matching while suppressing performance degradation of the maximum available gain and minimum noise figure. The developed low-noise amplifier MMIC, which implements simple matching circuits by using biasing elements as matching elements, had a linear gain of more than 21.4 dB and a noise figure of less than 1.91 dB in the wide bandwidth of 4.3–7.4 GHz. Under the single-tone power test, the low-noise amplifier MMIC had an output P1dB of 14.3–20.1 dBm, and the two-tone intermodulation distortion measurement exhibited an input third-order intercept point (IIP3) of 2.2–5.6 dBm in the same frequency range as the above.

Key Words: GaN HEMT, Gate-Drain Shunt Feedback, Inductive Source Degeneration, Low-Noise Amplifier, MMIC.

I. Introduction

In the past, radar receiver modules mostly used GaAs pHEMT (pseudomorphic high electron mobility transistor) low-noise amplifiers because they have a highly efficient power performance due to low voltage operation and a high driving current capability and exhibit high operation frequency from their inherent high electron mobility. RF input signals in a transmitter module are amplified in a high-power amplifier and are radiated through an antenna, but some of the transmitting signals are reflected from the antenna and enter a receiver module. Depending on their power level, such leaked or reentered signals may cause malfunctions in or fatal damage to the receiver module. To prevent these unwanted operation results and protect the receiver module from outside high-power signals, an additional protection circuit, such as a limiting circuit, is required to cut off the leaked signals from the transmitter or to at least reduce their signal magnitude. The additional circuit, placed in front of a low-noise amplifier in the receiver module, increases the module size and degrades the noise figure of the receiver system [1–4].

To overcome these limitations, many recent studies have been conducted on RF receiver modules using GaN HEMTs. Because a GaN HEMT has larger breakdown voltage, superior linearity

Manuscript received April 18, 2022 ; Revised July 1, 2022 ; Accepted August 28, 2022. (ID No. 20220418-047J)
[1]Department of Radio and Information Communications, Chungnam National University, Daejeon, Korea.
[2]Defense Materials and Components Convergence Research Department, Electronics and Telecommunications Research Institute (ETRI), Daejeon, Korea.
[*]Corresponding Author: Dong-Wook Kim (e-mail: dwkim21c@cnu.ac.kr)

at a high-power operation mode, high electron mobility, and high thermal conductivity compared with Si and GaAs devices, we did not need additional protection circuits for receiver protection. In addition, using a GaN HEMT instead of Si or GaAs devices in the receiver module has sufficient merits in terms of module compactness and system noise performance [5–9]. In this paper, we present designed and measured results of a C-band GaN dual-feedback low-noise amplifier MMIC with high robustness based on the 0.2 μm GaN HEMT process of the Electronics and Telecommunications Research Institute (ETRI).

II. Design of C-Band GaN Low-Noise Amplifier MMIC

1. GaN HEMT

In this work, S-parameter data for a GaN HEMT with gate fingers of 4 μm × 100 μm, which is measured up to 26 GHz at the bias conditions of $V_{GS} = -3.5$ V, $V_{DS} = 20$ V, and $I_{DS} =$ 40 mA, were used for simulations. The S-parameter data show that the maximum available gain is 15.5–18.4 dB and the minimum noise figure is 0.47–0.78 dB in the C-band frequency region, with the reference planes on the gate and drain pads. The cutoff frequency f_t and the maximum oscillation frequency f_{max} of the transistor were extrapolated from the S-parameter data and were estimated to be 31.7 GHz and 70.3 GHz, respectively.

Table 1 shows the design specifications of a C-band low-noise amplifier MMIC that requires a linear gain of 21 dB or more and a noise figure of 2 dB or below in 5–6 GHz. We used measured noise parameters in the S-parameter data file for noise simulation, and, for linear simulation, applied an equivalent inductor model, which was extracted from electromagnetic momentum simulation, and an equivalent capacitor model, which was based on the dielectric properties of the ETRI HEMT process.

2. Circuit Stabilization

A low-noise amplifier requires a stability factor larger than 1 both within and outside the design frequency band to prevent unwanted circuit instability. However, the S-parameter simulation results of the transistor showed that it was unstable at the bias conditions of $V_{GS} = -3.5$ V, $V_{DS} = 20$ V, and $I_{DS} = 40$ mA. To measure the circuit with no oscillation, we first stabilized the transistor and then proceeded with a design and simulation procedure of the matching circuits for the noise/gain matching. The stabilized circuit for the transistor is shown in Fig. 1 and has a configuration of a source feedback inductor L_S and a gate-drain shunt feedback RC circuit of the resistor R_F and the capacitor C_F.

Fig. 2 shows the variation of input, output, and optimum noise impedance traces via the dual-feedback effect on a Smith chart when the transistor is stabilized with the help of the source inductive feedback and the RC gate-drain shunt feedback in Fig. 1. The source inductor L_S, which was implemented using a microstrip line, improves circuit stability in a higher frequency region of the operation bandwidth and moves the impedances at the gate and drain ports of the transistor to the impedance region close to 50 Ω, thus making it easy to obtain

Table 1. Design specifications of the C-Band GaN low-noise amplifier MMIC

Parameter	Value
Frequency (GHz)	5–6
Associated gain (dB)	≥21
Noise figure (dB)	≤2
Input return loss (dB)	≥10
Size (mm)	≤1.7 × 1.7

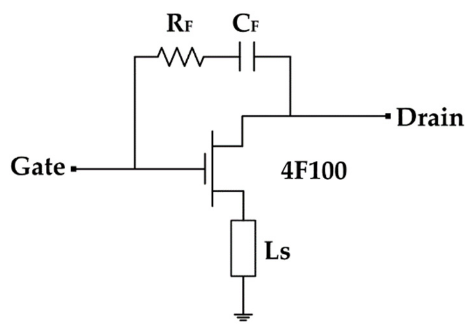

Fig. 1. Circuit stabilization using the inductive source feedback and the gate-drain RC shunt feedback.

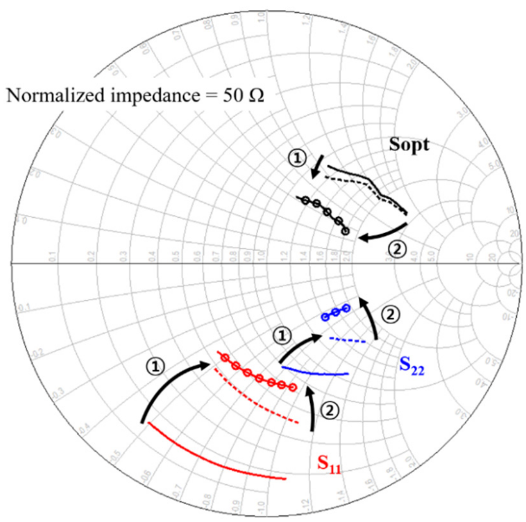

Fig. 2. Variation of the input, output, and optimum noise impedance traces via the dual-feedback effect (① inductive source feedback, ② gate-drain shunt feedback).

compromised matching traces for the input impedance matching, optimum noise matching (S_{opt}), and output impedance matching. The gate-drain shunt feedback circuit of R_F and C_F improves stability in the lower frequency band and moves the impedance traces to the impedance region where the impedance matching is possible only with a small number of passive elements. Considering the trace of S_{22}, the output impedance matching can be implemented only with an inductive shunt drain bias line and a blocking capacitor. The movement of the impedance traces via dual feedback makes it easier to achieve wideband matching and reduces the chip area by decreasing the number of passive matching elements. While the feedback circuits of the transistor provide advantages in terms of choosing the input impedance and optimum noise impedance and securing circuit stability, they degrade the available gain and noise figure. To reduce this degradation, we used a minimum-length microstrip line at the transistor source to provide a minimum stability factor in the design frequency range, and the same approach was applied to the gate-drain feedback circuit for the optimum combination of R_F and C_F. The width and length of the microstrip lines at the source ports of the transistors in the first stage and the second stage were 17 μm/250 μm and 25 μm/130 μm, respectively, and the resistors and capacitors of the first and second stages were 0.5 pF/1.3 kΩ and 2.5 pF/0.5 kΩ, respectively.

3. Input, Output, and Noise Matching Circuit Design

To achieve the design specifications in Table 1, we used a dual-feedback two-stage configuration for a C-band amplifier MMIC.

Fig. 3 shows a schematic circuit diagram of the proposed C-band GaN low-noise amplifier. When the transistor was stabilized by the dual-feedback structure in the C-band frequency region, the optimum source impedance for the maximum available gain and the optimum noise impedance for the minimum noise figure of the first-stage transistor were $Z_{S,GAIN}$ = 14.87 + *j*38.23 Ω and $Z_{S,NOISE}$ = 81.75 + *j*31.06 Ω at 5 GHz. The expected available gain was 14.9 dB at the optimum source impedance, and the expected noise figure was 1.03 dB at the optimum noise impedance. To proceed with the circuit design, we needed a compromised impedance for the gain, noise figure, and input return loss, which we found was 35.05 + *j*20.28 Ω at 5 GHz. The simulation showed a linear gain of about 13 dB, a noise figure of 1.3 dB, and an input return loss of more than 10 dB at the compromised source impedance. After the input impedance, the optimum gain impedance and optimum noise impedance of the second-stage transistor were investigated in the same manner, with a newly compromised impedance of 34.61 + *j*25.93 Ω being drawn at 5 GHz. Using the source and load impedances extracted from each stage, we designed the input matching circuit of the first stage and the output matching circuit of the second stage, and we then implemented the interstage matching circuit between the first stage and the second stage with the input and output matching circuits attached.

To minimize the number of passive matching elements in the input and output matching circuits, the matching circuits were composed of inductive drain bias lines, DC blocking capacitors, and microstrip lines for the interconnection between passive elements. The interstage matching circuit can provide additional low-frequency stability by introducing an intentional low-frequency mismatch, one which decreases the low-frequency gain while maintaining noise performance.

Because the gate and drain bias conditions of the first stage were the same as those of the second stage, we used a gate bias pad and a drain bias pad for the two stages and added a gate bias resistor of 270 Ω and a drain bias resistor of 2.5 Ω to suppress a potential loop feedback oscillation through the pads between the stages. Also, to prevent unpredictable low-frequency oscillation, we inserted RC shunt traps into the bias lines. Fig. 4 shows the designed impedance traces of the input, interstage, and output matching circuits.

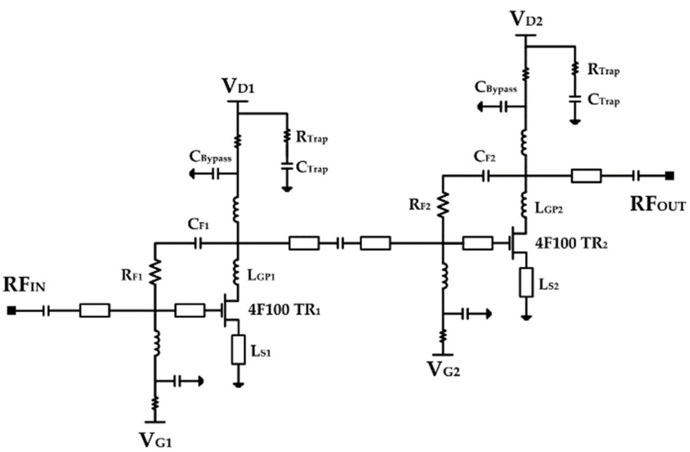

Fig. 3. Schematic circuit diagram of the proposed C-band GaN low-noise amplifier.

III. MEASUREMENT RESULTS

Fig. 5 shows a photograph of the C-band low-noise amplifier MMIC that was fabricated using the 0.2 μm GaN HEMT process of ETRI. The chip occupies an area of 1.62 mm × 1.62 mm, including RF and DC pads whose positions were fixed for the direct connection of a whole transceiver chip. The bare chip was attached on an Al carrier using a silver epoxy for on-wafer measurement.

Fig. 6 shows simulated and measured *S*-parameters at V_{DS} = 20 V and I_{DS} = 41 mA. The on-wafer measurement was accomplished using a cascade on-wafer probe system and a

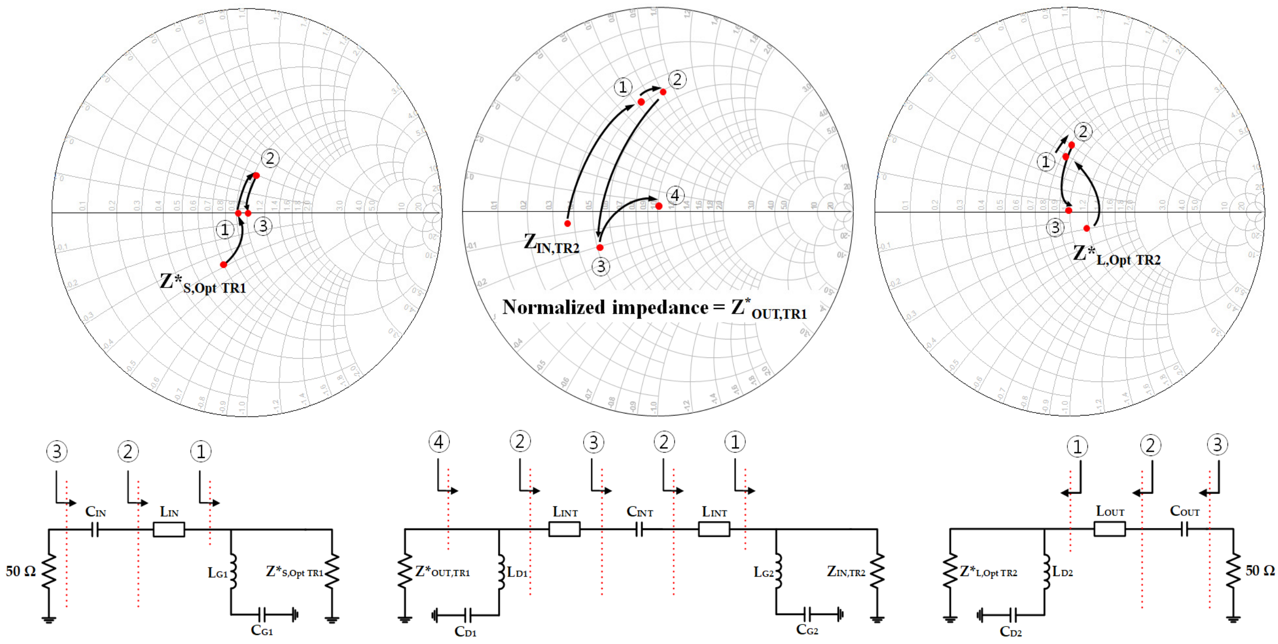

(a) (b) (c)

Fig. 4. Impedance traces of the input, interstage, and output matching circuits: (a) input impedance trace, (b) interstage impedance trace ($Z_{OUT,TR1} = 62.2 - j23.2\ \Omega$), and (c) output impedance trace.

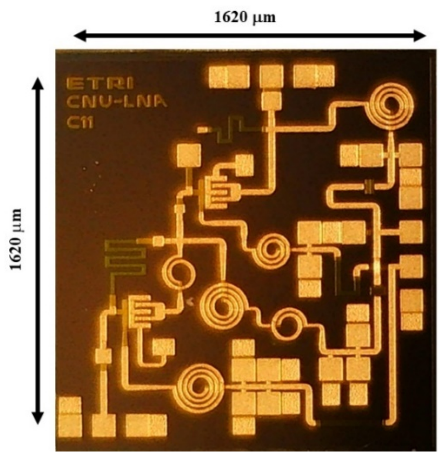

Fig. 5. Photograph of the fabricated C-band low-noise amplifier MMIC chip.

Keysight network analyzer (model N5230). The measured S_{21} was 23.9 dB at 6 GHz, which had a very small difference of 0.2 dB compared with the simulated S_{21} of 24.1 dB. The measurement demonstrated a linear gain of more than 21 dB, an input return loss of more than 9.5 dB, and an output return loss of more than 12.2 dB, from 4.3 GHz to 7.4 GHz. Overall, compared with the simulated results, the measured gain and input return loss shifted upward by about 0.5 GHz, and the input return loss was slightly degraded.

Fig. 7 compares the measured noise figure of the fabricated low-noise amplifier with its simulated noise figure. A Keysight noise analyzer (model N8975A) and noise source (model N4002A) were used for the noise measurement, and RF probes

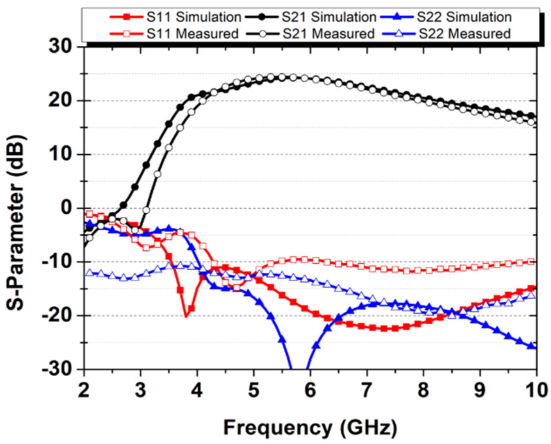

Fig. 6. Comparison of the simulated and measured S-parameter results.

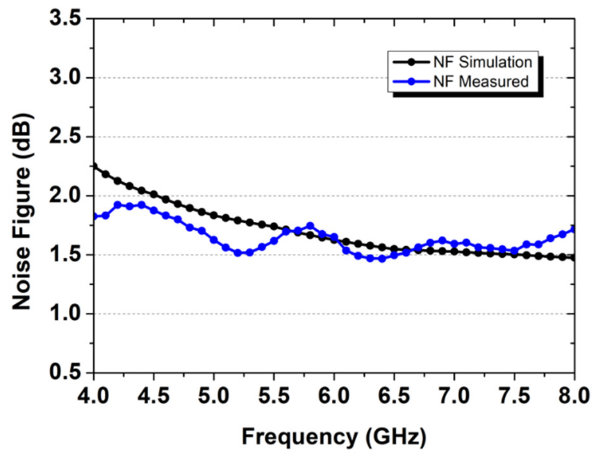

Fig. 7. Comparison of the simulated and measured noise figures.

and cables for the measurement were de-embedded using their own S-parameters to extract the noise figure of the low-noise amplifier itself. The simulated and measured noise figures were 1.63 dB and 1.65 dB at 6 GHz. The latter had a ripple of 0.16 dB, which was caused partly by the measurement process in an open—not shielded—environment. Overall, the measured noise figure was less than 2 dB in the C-band frequency region. The measured noise figure exhibited frequency downshifts from the simulated results, which was a characteristic opposite to those of the gain and input return loss. This is because the input impedance trace moved closer to the optimum noise impedance rather than to the optimum gain impedance, which could be identified through the improvement of the noise figure in a lower frequency band.

Fig. 8 shows the variation of the output power and power gain with the input power at 6 GHz, which had an output 1dB compression point (P1dB) of 19.4 dBm and a power gain of 22.4 dB at P1dB.

The third-order intermodulation distortion (IMD3) measurement was performed using two Keysight signal generators (model E8267D and E8257D) and a spectrum analyzer (model E4446A) from 4.5 GHz to 6.5 GHz, with the frequency step of 0.5 GHz. Fig. 9 shows the measured IMD3 output power at 6 GHz, with two-tone input signals of f_{LOW} = 6.05 GHz and f_{HIGH} = 6.1 GHz applied. The output power at f_{HIGH} and the high-band IMD3 are not displayed because they are the same as those in Fig. 9. As shown in Fig. 9, the IMD3 measurement demonstrated an output third-order intercept point (OIP3) of 25.9 dBm, which corresponded to an input third-order intercept point (IIP3) of 2.5 dBm.

Table 2 shows the measured results of the power gain, P1dB, IIP3, and OIP3 from 4.5 GHz to 6.5 GHz with the frequency step of 0.5 GHz. P1dB was measured to be 16 dBm or more, and OIP3 was measured to be 25.5 dBm or more, in a whole frequency region, except at 4.5 GHz.

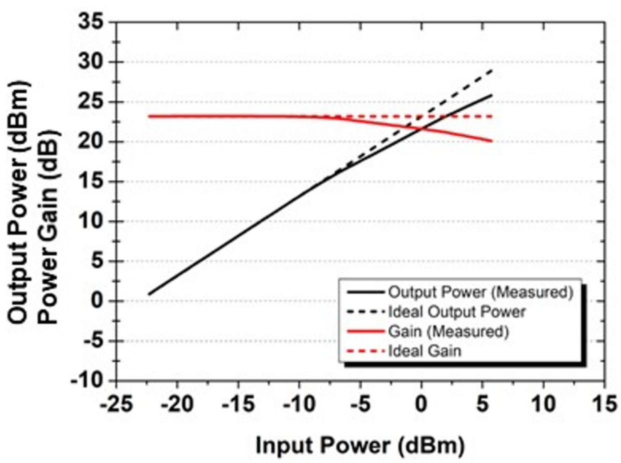

Fig. 8. Variation of the output power and power gain of the low-noise amplifier with the input power (f_O = 6 GHz).

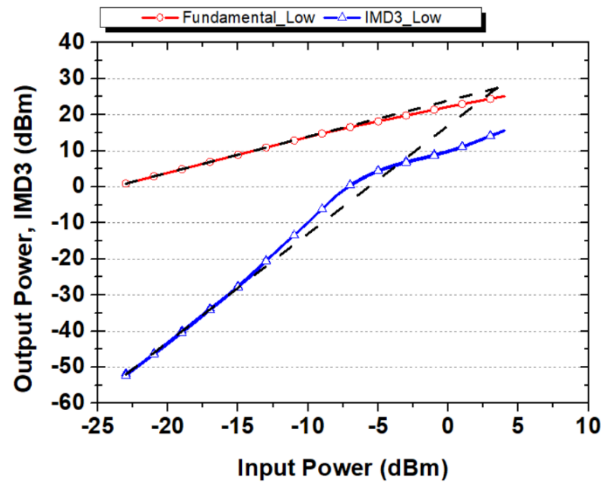

Fig. 9. Measured third-order intermodulation (IMD3) results of the low-noise amplifier at 6 GHz with two-tone input signals (f_{LOW} = 6.05 GHz, f_{HIGH} = 6.1 GHz, Δf = 50 MHz).

Table 2. Measured results of the power gain, P1dB, IIP3, and OIP3 with the frequency

Frequency (GHz)	Power gain (dB)	P1dB (dBm)	IIP3 (dBm)	OIP3 (dBm)
4.5	21.1	14.3	2.2	23.3
5	22.8	16	2.7	25.5
5.5	23.7	17.5	2.4	26.1
6	23.4	19.4	2.5	25.9
6.5	22.5	20.1	5.6	28.1

Table 3 compares our results with those of previously published C-band low-noise amplifiers [10–15]. Our fabricated C-band low-noise amplifier MMIC demonstrated better gain performance than [12] and [14] while maintaining a similar size, and also showed performance similar to [11] and [13], but achieved a size reduction of 46% and 27%, respectively. Therefore, our work shows comparable or superior performance in terms of the bandwidth, gain, noise figure, and chip area, compared with other previously published works.

IV. Conclusion

In this work, a C-band low-noise amplifier MMIC was designed and fabricated using the ETRI's 0.2 μm GaN HEMT MMIC process. By obtaining stability in both the low-frequency and high-frequency regions with the dual feedback of the inductive source feedback and the RC gate-drain shunt feedback, and by implementing a simple matching circuit for the compromised impedance trace of the input/output gain matching

Table 3. Comparison of our work and the previously published C-band low-noise amplifier results

Study	Frequency (GHz)	Gain (dB)	Noise figure (dB)	Input return loss (dB)	P1dB (dBm)	OIP3 (dBm)	Chip area (mm^2)	Process
Andrei et al. [10]	5–6	≥ 12	5.5	7–14	N/A	N/A	N/A	GaN HEMT
Shih et al. [11]	2–5	17.4	1.5–2	7–10	20	N/A	4.86	GaN HEMT
Abounemra et al. [12]	5–6	14	1.3–1.6	12–14.6	22	35	2.55	GaN HEMT
Abounemra et al. [13]	4.5–7	22.5–25.5	1.3–1.8	9–15	24	35	3.6	GaN HEMT
Han and Kim [14]	2–12	15	≤ 3	≥ 13	N/A	20	2.9	GaN HEMT
Bassal and Jarndal [15]	1–6	14	2.9	2.44	N/A	43	N/A	GaN HEMT
This work	4.3–7.4	21.4–24.4	1.47–1.91	9.5–14.8	14.3–20.1	23.3–28.1	2.62	GaN HEMT

and optimum noise matching, we reduced the loss of the matching circuits and achieved wideband performance together with the small chip area. The fabricated low-noise amplifier MMIC had an operation bandwidth of 4.3–7.4 GHz, which is wider than the original design bandwidth of 5–6 GHz, and achieved a linear gain of 21.4–24.4 dB, a noise figure of 1.47–1.91 dB, and an input return loss of 9.5–14.8 dB. The power measurement showed that the output P1dB was 14.3–20.1 dBm, while the IIP3 was 2.2–5.6 dBm. The fabricated amplifier can be effectively used for radar receiver components and modules that should be able to endure high input power and require a small form factor.

This work was supported by the National Research Council of Science and Technology (NST) grant by the Korea government (MSIT) (No. CRC-19-02-ETRI).

References

[1] C. V. Rao, D. K. Ghodgaonkar, and N. Sharma, "GaAs MMIC low noise amplifier with integrated high-power absorptive receive protection switch," *IEEE Microwave and Wireless Components Letters*, vol. 28, no. 12, pp. 1128-1130, 2018.

[2] A. Barigelli, W. Ciccognani, S. Colangeli, P. Colantonio, M. Feudale, F. Giannini, et al., "Development of GaN based MMIC for next generation X-band space SAR T/R module," in *Proceedings of 2012 7th European Microwave Integrated Circuit Conference*, Amsterdam, Netherlands, 2012, pp. 369-372.

[3] M. Thorsell, M. Fagerlind, K. Andersson, N. Billstrom, and N. Rorsman, "An X-band AlGaN/GaN MMIC receiver front-end," *IEEE Microwave and Wireless Components Letters*, vol. 20, no. 1, pp. 55-57, 2010.

[4] S. D'Angelo, A. Biondi, F. Scappaviva, D. Resca, and V. A. Monaco, "A GaN MMIC chipset suitable for integration in future X-band spaceborne radar T/R module frontends," in *Proceedings of 2016 21st International Conference on Microwave, Radar and Wireless Communications (MIKON)*, Krakow, Poland, 2016, pp. 1-4.

[5] M. Chen, W. Sutton, I. Smorchkova, B. Heying, W. B. Luo, V. Gambin, et al., "A 1–25 GHz GaN HEMT MMIC low-noise amplifier," *IEEE Microwave and Wireless Components Letters*, vol. 20, no. 10, pp. 563-565, 2010.

[6] M. P. Lee, S. Kim, S. J. Hong, and D. W. Kim, "Compact 20-W GaN internally matched power amplifier for 2.5 GHz to 6 GHz jammer systems," *Micromachines*, vol. 11, no. 4, article no. 375, 2020. https://doi.org/10.3390/mi11040375

[7] S. Zhang, P. Zheng, J. Xu, R. Wang, Y. Huang, and X. Tong, "A 15–34 GHz robust GaN based low-noise amplifier with 0.8 dB minimum noise figure," in *Proceedings of 2019 17th IEEE International New Circuits and Systems Conference (NEWCAS)*, Munich, Germany, 2019, pp. 1-4.

[8] M. Rudolph, R. Behtash, R. Doerner, K. Hirche, J. Wurfl, W. Heinrich, and G. Trankle, "Analysis of the survivability of GaN low-noise amplifiers," *IEEE Transactions on Microwave Theory and Techniques*, vol. 55, no. 1, pp. 37-43, 2007.

[9] S. Zafar, S. Osmanoglu, B. Cankaya, A. Kashif, and E. Ozbay, "GaN-on-SiC LNA for UHF and L-band," in *Proceedings of 2019 European Microwave Conference in Central Europe (EuMCE)*, Prague, Czech Republic, 2019, pp. 95-98.

[10] C. Andrei, O. Bengtsson, R. Doerner, S. A. Chevtchenko, and M. Rudolph, "Robust stacked GaN-based low-noise amplifier MMIC for receiver applications," in *Proceedings of 2015 IEEE MTT-S International Microwave Symposium*, Phoenix, AZ, 2015, pp. 1-4.

[11] S. E. Shih, W. R. Deal, W. E. Sutton, Y. C. Chen, I.

Smorchkova, B. Heying, M. Wojtowicz, and M. Siddiqui, "Broadband GaN dual-gate HEMT low noise amplifier," in *Proceedings of 2007 IEEE Compound Semiconductor Integrated Circuits Symposium*, Portland, OR, 2007, pp. 1-4.
[12] A. E. Abounemra, M. Helaoui, and F. M. Ghannouchi, "A highly survivable C-band GaN HEMT LNA with resistive feedback technique," in *Proceedings of 2019 IEEE 19th Mediterranean Microwave Symposium (MMS)*, Hammamet, Tunisia, 2019, pp. 1-4.
[13] A. E. Abounemra, M. Helaoui, and F. M. Ghannouchi, "A high gain and high linear 0.25 μm GaN HEMT based monolithic integrated C-band low noise amplifier," in *Proceedings of 2019 IEEE International Electromagnetics and Antenna Conference (IEMANTENNA)*, Vancouver, Canada, 2019, pp. 16-19.
[14] J. H. Han and J. G. Kim, "A S/C/X-Band GaN low noise amplifier MMIC," *The Journal of Korean Institute of Electromagnetic Engineering and Science*, vol. 28, no. 5, pp. 430-433, 2017.
[15] A. M. Bassal and A. M. Jarndal, "GaN low noise amplifier design for WiMax applications," in *Proceedings of 2016 16th Mediterranean Microwave Symposium (MMS)*, Abu Dhabi, United Arab Emirates, 2016, pp. 1-4.

Ha-Wuk Sung

received B.S. and M.S. degrees in radio science and engineering from Chungnam National University, Daejeon, Republic of Korea, in 2021. He has been working for MMII Laboratory since 2022. His research interests include GaN HEMT power amplifier MMICs and low-noise amplifier MMICs.

Seong-Hee Han

received a B.S. degree in radio science and engineering from Chungnam National University, Daejeon, Republic of Korea, in 2021. He is currently an M.S. candidate in the same university. His research interests include mm-wave GaAs pHEMT power amplifier MMICs and 3D printing techniques for microwave components.

Seong-Il Kim

received his B.S. degree in electrical engineering from Hanyang University, Seoul, Republic of Korea, in 1998, his M.S. degree in electrical engineering from Korea Advanced Institute of Science and Technology (KAIST), Daejeon, Republic of Korea, in 2000, and his Ph.D. degree in electrical engineering from Chungnam National University, Daejeon, Republic of Korea, in 2019. Since 2000, he has been with the Electronics and Telecommunications Research Institute (ETRI), Republic of Korea, as a research staff member, where he has been engaged in research on optoelectronic digital IC design and RF power amplifier design. He is currently a director of the Defense RF Packaging Research Section. His main research interests are GaN HEMT device modeling and GaN MMIC design for transceiver modules.

Ho-Kyun Ahn

received his B.S. and M.S. degrees in material science and engineering from Korea University, Seoul, Republic of Korea, in 1999 and 2001, respectively. In 2001, he joined the Electronics and Telecommunications Research Institute (ETRI), where he has been engaged in research on compound semiconductor devices and MMICs. He received his Ph.D. degree in electronics from Kyungpook National University, Daegu, Republic of Korea, in 2016. He is currently a director of the Defense RF Components Research Section in ETRI. His current research interests include the fabrication and characterization of GaN-based devices and MMICs.

Jong-Won Lim

received B.S., M.S., and Ph.D. degrees in physics from Chung-Ang University, Seoul, Republic of Korea, in 1988, 1990, and 1998, respectively. In 2000, he joined the Electronics and Telecommunications Research Institute (ETRI) as a senior research staff member, where he has been engaged in research on MMIC development for communications. Since 2019, he has been a managing director of the Defense Materials and Components (DMC) Convergence Research Department in ETRI. His current research interests include the process development, fabrication, and characterization of GaN-based HEMT devices and MMICs for millimeter-wave applications.

Dong-Wook Kim

received his B.S. degree in electronic communications from Hanyang University, Seoul, Republic of Korea, in 1990, and his M.S. and Ph.D. degrees in electrical engineering from Korea Advanced Institute of Science and Technology (KAIST), Daejeon, Republic of Korea, in 1992 and 1996, respectively. In 1996, he joined the LG Electronics Research Center, Seoul, Republic of Korea, where he developed high-power III–V semiconductor devices and monolithic microwave integrated circuits until 2000. From 2000 to 2002, he led R&D teams to develop RF integrated passive devices on a thick oxidized Si substrate and their applications as a director of the R&D center in Telephus Inc. From 2002 to 2004, he was involved in the development of wireless security systems as a team leader at S1 Corporation, a company of the Samsung Group. In 2004, he joined the faculty of Chungnam National University, Daejeon, Republic of Korea. In 2009, he was also with ETRI as an invited researcher. In 2010, he was a visiting scholar at the University of California at San Diego, La Jolla. He was the director of the Center for Information and Communication in Chungnam National University from 2016 to 2018, and is currently a full professor and also the director of the Radiowave and Electrical Engineering Research Center. He has been an IEEE senior member since 2017. His research interests are GaAs- and GaN-based MMICs, internally matched power amplifiers, and microwave/millimeter-wave embedded modules, including miniaturized radar/sensor modules and ultra-wideband high-power modules.